Error Propagation in Geometric Constructions

J. Wallner[a], R. Krasauskas[b], H. Pottmann[a]

[a] *Institut für Geometrie, TU Wien, Wiedner Hauptstraße 8–10, A-1040 Wien, Austria*
[b] *Department of Mathematics, Vilnius University, Naugarduko 24, LT-2600 Vilnius, Lithuania.*

Abstract

In this paper we consider error propagation in geometric constructions from a geometric viewpoint. First we study affine combinations of convex bodies: This has numerous examples in splines curves and surfaces defined by control points. Second, we study in detail the circumcircle of three points in the Euclidean plane. It turns out that the right geometric setting for this problem is Laguerre geometry and the cyclographic mapping, which provides a point model for sets of circles or spheres.

Keywords: Error propagation, convex combination, spline curve, Apollonius problem.

1 Introduction

The aim of this paper is to show how to treat some problems of error propagation in geometric constructions in a geometric way.

A *geometric construction* is a procedure which takes geometric objects (points, lines, circles) as input, and gives a geometric object as output. It must be *invariant* with respect to some geometry, which is best explained by an example:

We consider a very simple geometry construction: the intersection of two lines in the Euclidean plane. The input consists of two lines, and the output is a point. If we translate or rotate the input data, the output undergoes the same transformation. This means invariance with respect to Euclidean transformations.

If we speak of *error propagation*, we mean the following: Suppose each item of the input data can vary independently in some domain (for instance, a point varies in a disk). We can think of input data given imprecisely or of *tolerance zones* for the input data. We ask for the set of all possible outputs. If this is not possible, we would at least want to know some tolerance zone which contains all possible outputs (cf. [13]).

From the geometric point of view, we want *precise* answers to these questions which are again geometric invariants and do not not contain artifacts of a coordinatization. The computational viewpoint includes more than that, e.g., the complexity of algorithms. One might be more interested in a faster computation which gives looser error bounds. Here we discuss the computation of exact tolerance zones.

Interval arithmetic

Interval arithmetic (see [2, 7, 8, 17, 18, 19]) is one of the basic tools, if one has bounds for input data of some calculations, and wants to compute bounds for the output. A simple example shows how interval arithmetic is not 'geometric' in the sense that it does not give exact error bounds:

Suppose the point (x,y) has coordinates $x \in [1-\varepsilon, 1+\varepsilon]$, $y \in [-\varepsilon, \varepsilon]$. If we rotate this point about 45 degrees, we know its image (x', y') to have coordinates $x', y' \in [\sqrt{2}/2 - \sqrt{2}/2 \cdot \varepsilon, \sqrt{2}/2 + \sqrt{2}/2 \cdot \varepsilon]$. If we know only the bounds for x', y' independently, a further rotation about 45 degrees gives the point (x'', y'') whose coordinates are bounded by $x'' \in [-2\varepsilon, 2\varepsilon]$, $y'' \in [1-2\varepsilon, 1+2\varepsilon]$, whereas rotation of (x,y) about 90 degrees gives the bounds $x'' \in [-\varepsilon, \varepsilon]$, $y'' \in [1-\varepsilon, 1+\varepsilon]$.

A computational scheme which handles error bounds and tolerances in a *geometric* way is expected to rotate the tolerance square of the point (x,y), but never to increase its size.

Nevertheless in Sec. 2.4 we show that interval arithmetic fits in a natural way into our approach.

Special problems

In this paper we restrict ourselves to two different types of problems: First, we consider geometric constructions which are affine or even convex combinations of points, which is a geometric operation in *affine geometry* — if the input data undergo an affine transformation, the output does the same.

This includes most of the spline curves defined by control points. We assume that the control points can vary independently in closed convex domains: For a parameter value t we look for the locus of possible curve points. We will always assume that the error pertinent in the computation of the curve point is negligible in comparison to the effect of changing the control points in their various domains. So the problem reduces to the problem of affine or convex combination of planar or spatial domains.

As a second example we consider an elementary Euclidean geometric construction: the circumcircle of three points. The difference between these two is that the former is affinely invariant, involving only the linear structure of real vector space $\mathbb{R}^n$, whereas the latter is a Euclidean construction which involves the Euclidean orthogonality relation and metric.

In general, metric constructions are not as easy to analyze as affine ones. A detailed algorithmic study of geometric constructions involving lines and circles is given by [6]. Applications to collision problems involving toleranced objects are studied in [1]. Nevertheless there is still much to do in this field.

Another topic is the inverse problem: Given a geometric construction and a tolerance domain, how must we choose the input tolerances?

2 Linear combinations of control points and applications to spline curves.

2.1 Elementary facts about convex bodies

One of the main tools for studying compact convex bodies of $\mathbb{R}^d$ is the *support function*. There is large amount of literature including some monographs (see e.g. [9] for a detailed overview of the whole field of convex geometry). For the convenience of the reader we repeat some basic facts.

We call a plane ε a *support plane* of K if K has a point in common with ε and K is entirely contained in one of the two closed half-spaces defined by ε. For all unit vectors n there is a unique plane $\varepsilon(n)$ orthogonal to n which is a support plane of K such that K lies in the half-space indicated by $-n$ and bounded by $\varepsilon(n)$. The oriented distance of this plane to the previously fixed origin is the value of the support function $s(n)$. Then ε has the equation $x \cdot n = s(n)$ and K lies in the half-space $x \cdot n \leq s(n)$.

The domain of a support function is the unit sphere S^{d-1} of $\mathbb{R}^d$. In the plane ($n = 2$) it is sometimes useful to make the domain of the support function the interval $[0, 2\pi]$ or even the entire real line, where an angle ϕ is identified with the appropriate point of the unit circle. We will never do this, because we sometimes evaluate the support function at vectors n and $-n$, which are opposite points of the unit sphere. In the case $n = 2$ opposite points correspond to angles $\phi, \phi + \pi$, and $-\phi$ means something different. In order to avoid confusion, let us state explicitly that the minus sign always indicates the *opposite point* of the unit sphere.

If K is a convex body, λK is the set of all $\lambda \cdot x$ with $x \in K$. For two convex bodies K_1, K_2 we define their sum $K = K_1 + K_2$ as the set of all $x_1 + x_2$ with $x_1 \in K_1$, $x_2 \in K_2$. This sum operation is called *Minkowski sum* (see e.g. [10]).

For real numbers t_1, t_2 we then can define the body $K = t_1 K_1 + t_2 K_2$. Especially we define *affine combinations* $(1-t)K_1 + tK_2$ of convex bodies, and *convex combinations*, which are affine combinations with $0 \leq t \leq 1$.

Among the basic properties of support functions are the following: If $s : S^{d-1} \to \mathbb{R}$ is the support function of K, then $K' = \lambda K$ has the support function $s'(n) = \lambda \cdot s(n)$ if $\lambda \geq 0$. The support function s' of $-K$ is given by $s'(n) = s(-n)$. If s_1, s_2 are the support functions of K_1, K_2, resp., and $0 \leq t \leq 1$, then the convex body $K = (1-t)K_1 + tK_2$ has the support function $s = (1-t)s_1 + ts_2$. This is clear from close inspection of Fig. 1, which illustrates the fact that the boundaries of K_1, K_2, K can be seen as projection of three closed curves in parallel planes, the middle curve thereby lying on the unique embedded developable surface which joins the other two. From this easily follows that the support function of the convex body $\lambda_1 K_1 + \lambda_2 K_2$ equals $\lambda_1 s_1 + \lambda_2 s_2$ if both λ_1, λ_2 are nonnegative.

As an application of this, we derive the support function s of a linear combination $K = \sum \lambda_i K_i$ of convex bodies K_i with support functions s_i.

$$K = \sum_{\lambda_i > 0} \lambda_i K_i + \sum_{\lambda_i < 0} \lambda_i K_i. = \sum_{\lambda_i > 0} \lambda_i K_i + \sum_{\lambda_i < 0} (-\lambda_i)(-K_i).$$

The support function s_i' of $-K_i$ is given by $s_i'(n) = s_i(-n)$. Clearly, the support function of a *positive* linear combination of convex bodies is the same linear combination of their support functions. Thus

$$s(n) = \sum_{\lambda_i > 0} \lambda_i s_i(n) + \sum_{\lambda_i < 0} (-\lambda_i) s_i(-n).$$

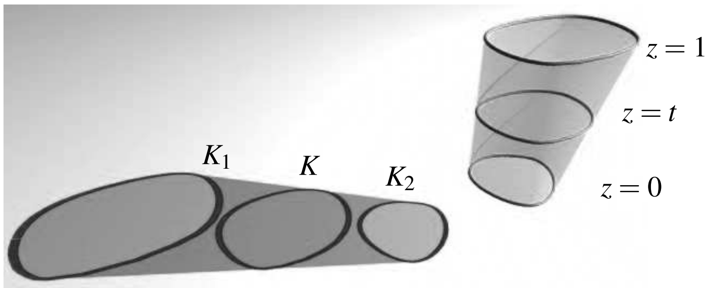

Figure 1: Developable surface and convex combination $K = (1-t)K_1 + tK_2$ of convex domains

If we know the support function of a convex body, we can determine its diameters: The distance between supporting planes with normal vectors n and $-n$ is called the *diameter* $d_n(K)$ of the convex body K 'in direction n'. Clearly

$$d_n(K) = |s(n) - s(-n)|.$$

If K is a convex combination $K = \sum \lambda_i K_i$, then so is the support function, and we have

$$d_n(K) = \sum \lambda_i d_n(K_i),$$

i.e., the diameter of K is the appropriate convex combination of the diameters of the convex bodies K_i. Because the diameter is an indicator of the extent of a convex body in space, this is useful to know.

We should mention that many other properties of convex bodies (such as perimeter or surface area) can also be expressed in terms of the support function.

2.2 Curves and surfaces defined by control points

Many curve and surface schemes in Computer Aided Geometric Design consist, in principle, of *affine* or *convex* combinations of control points. Convex combinations are especially simple because all coefficients are positive. Important examples are the following:

• Bézier curves: $b(t) = \sum B_i^n(t) b_i$ where $B_i^n(t)$ is the i-th Bernstein polynomial of degree n. This sum is a convex combination if $0 \le t \le 1$.

• B-spline curves: $b(t) = \sum N_{i,T}^n(t) b_i$ where $N_{i,T}^n$ is the i-th normalized B-spline function of degree n defined by the knot vector T. This is a convex combination involving at most $n+1$ control points.

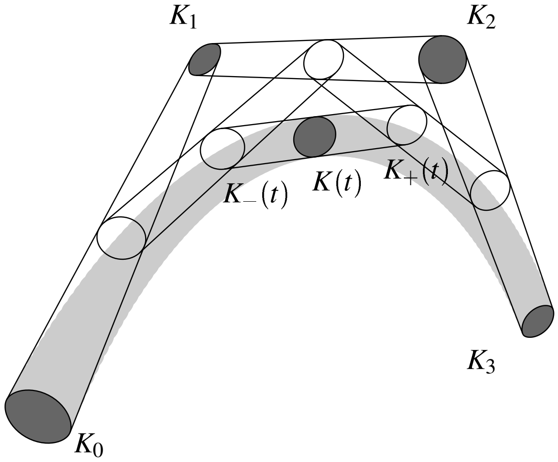

Figure 2: Bézier curve $\sum b_i B_i(t)$ with $0 \le t \le 1$

• The general L-spline spaces defined by a differential operator have bases of positive functions if certain conditions are met, so they fit here also.

• Interpolatory schemes are often linear as well. An example of this is interpolation with C^2 cubic B-splines, which is discussed later.

• Tensor product surfaces (TP surfaces) defined by two curve schemes with basis functions A_i, B_i by $b(u,v) = \sum_{i,j} A_i(u) B_j(v) b_{ij}$ give convex combinations if both curve schemes do so.

Examples are TP Bézier surfaces in the interior of the base rectangle, and TP B-spline surfaces.

• Denote the triangular Bernstein polynomials by $B_{i_0 i_1 i_2}(x)$. The point

$$b(x) = \sum_{i_0+i_1+i_2=n} b_{i_0 i_1 i_2} B_{i_0 i_1 i_2}(x),$$

of the triangular Bézier surface defined by control points $b_{i_0 i_1 i_2}$ is an affine combination of the control points and a convex combination in the interior of the base triangle (see later).

Bézier curves

Bézier curves and surfaces are defined as linear combinations of points with various different types of Bernstein polynomials. Only in some subset of the parameter domain all coefficients are positive. In the following we will describe the signs of the coefficient functions in different subsets of the parameter domain, and the resulting support

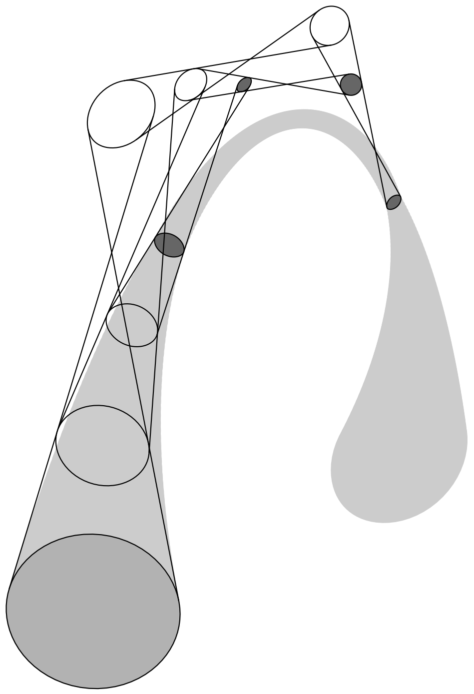

Figure 3: Bézier curve $\sum b_i B_i(t)$ with $-1/2 \leq t \leq 3/2$

functions of the appropriate linear combinations of convex bodies. We use the following notation: A control point b_i of a curve/surface corresponds to a convex body K_i, which has support function s_i. For multi-indices we will use an appropriately modified notation.

The sign of the ordinary Bernstein polynomials is given by

$$\operatorname{sgn}(B_i^n(t)) = \operatorname{sgn}(t)^{n-i}\operatorname{sgn}(1-t)^i$$

and so the support function s of the convex body $K = \sum B_i^n(t) K_i$ is given by

$$s(n) = \sum B_i^n(t) s_i^\star(n),$$

where

$$s_i^\star(n) = \begin{cases} s_i(n) \text{ for} & t<0,\ n-i \text{ even, or} \\ & t>1,\ i \text{ even, or} \\ & 0 \leq t \leq 1 \\ -s_i(-n) & t<0,\ n-i \text{ odd, or } t>1,\ i \text{ odd.} \end{cases}$$

This can be symbolized by the following diagram, where the filled circles indicate positive coefficients:

○●○●○●○●	●●●●●●●●	●○●○●○●○
$t<0$	$0<t<1$	$1<t$

Fig. 2 and Fig. 3 show the union of all possible K's when t ranges in an interval (shaded area). It is clearly seen that only in the case $0 \leq t \leq 1$ the diameter of the domain $K(t)$ is a convex combination of the diameters of the domains K_i: If $t \notin [0,1]$, the diameter of $K(t)$ is rapidly increasing. This illustrates the fact the often cited 'optimality' of the Bernstein basis is valid only in the interval $[0,1]$ (see [5]).

C^2 cubic spline interpolation

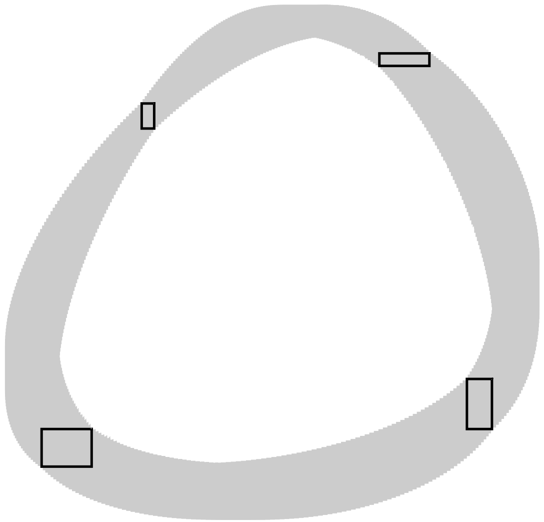

Figure 4: Interpolating 'interval' C^2 cubic B-spline

Assume we have points $x_0,\ldots,x_{L-1}$ and look for a C^2 cubic B-spline curve $s(u)$ with $s(i) = x_i$, and $s(t+L) = s(t)$. This means we have to find a cubic C^2 B-spline function $C(u)$ with the property that $C(0) = C(L) = C(2L) = \ldots = 1$ and $C(i) = 0$ for all other integers i. Then $\sum_{i=0}^{L-1} x_i C(t-i)$ is a solution. It is easily seen that the derivatives $C'(i)$ have to fulfill the equation

$$A \cdot \begin{pmatrix} C'(0) \\ \vdots \\ C'(L-1) \end{pmatrix} = \begin{pmatrix} C(1)-C(-1) \\ \vdots \\ C(L)-C(L-2) \end{pmatrix}$$

with

$$A = \begin{pmatrix} 4 & 1 & & & & 1 \\ 1 & 4 & 1 & & & \\ & 1 & 4 & 1 & & \\ & & \ddots & \ddots & & \\ 1 & & & & 1 & 4 \end{pmatrix}.$$

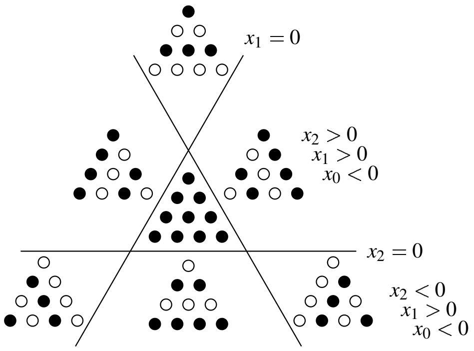

Figure 5: Distribution of signs of triangular Bernstein polynomials — see text for explanation.

The i-th row of the matrix A is obtained by appropriately shifting its first row (i.e., A is a circulant matrix). The inverse of A can be calculated and is again circulant. Its first row has, apart from some constant factor, the entries

$$a_i = (-1)^{i+1}(\alpha^{L-i} - \beta^{L-i} + (-1)^L(\alpha^i - \beta^i))$$

with $\alpha = 2+\sqrt{3}$, $\beta = 1/\alpha = 2-\sqrt{3}$. It is easy to see that the solution $C'(0), C'(1), \ldots$ has signs $(0, -, +, -, \ldots, [0], \ldots, -, +, -, +)$ where the 0 in brackets is inserted if and only if L is even. Clearly the signs of $C(u)$ in the intervals $[i, i+1]$, starting with $[0,1]$, are $+, -, +, -, \ldots$, with the exception that C has the same sign in the intervals $[L/2-1, L/2]$ and $[L/2, L/2+1]$ if L is even. This is discussed in [3].

As an example, we choose four rectangles and find all periodic interpolating cubic C^2 B-spline curves which pass through these rectangles. Because the locus of curve points for a certain parameter value t is not a convex combination of the basis rectangles, but only an affine one, its size increases if t is between the knots (see Fig. 4).

Triangular Bézier surfaces

Assume that x_0, x_1, x_2 are barycentric coordinates with respect to a triangle p_0, p_1, p_2 in the plane (i.e., the point designated by the coordinate triple $x = (x_0, x_1, x_2)$ with $\sum x_i = 1$ is the point $x_0p_0 + x_1p_1 + x_2p_2$). Then the triangular B-spline surface defined by control points $b_{i_0i_1i_2}$ in $\mathbb{R}^d$ ($i_0+i_1+i_2 = n$) is given by

$$b(x) = \sum_{i_0+i_1+i_2=n} b_{i_0i_1i_2} B_{i_0i_1i_2}(x)$$

where

$$B_{i_0i_1i_2} = \frac{(i_0+i_1+i_2)!}{i_0!i_1!i_2!} x_0^{i_0} x_1^{i_1} x_2^{i_2}.$$

This is an affine combination, as the sum of all $B_{i_0i_1i_2}$ equals 1, and it is clearly a convex combination if x is in the interior of the triangle $p_0p_1p_2$.

The sign of the basis function $B_{i_0i_1i_2}(x_0, x_1, x_2)$ is given by

$$\operatorname{sgn}(B_{i_0i_1i_2}(x_0,x_1,x_2) = \operatorname{sgn}(x_0)^{i_0} \operatorname{sgn}(x_1)^{i_1} \operatorname{sgn}(x_2)^{i_2}.$$

Thus the support function of the convex body $K = \sum_{i_0+i_1+i_2=n} B_{i_0i_1i_2}(x_0,x_1,x_2) K_{i_0i_1i_2}$ is given by

$$s(n) = \sum B_{i_0i_1i_2}(x_0,x_1,x_2) s^\star_{i_0i_1i_2}(n),$$

where

$$s^\star_{i_0i_1i_2}(n) = \begin{cases} s_{i_0i_1i_2}(n) & \text{if } \operatorname{sgn}(x_0^{i_0}x_1^{i_1}x_2^{i_2}) = 1 \\ -s_{i_0i_1i_2}(-n) & \text{if } \operatorname{sgn}(x_0^{i_0}x_1^{i_1}x_2^{i_2}) = -1. \end{cases}$$

This is depicted in a symbolical way in Fig. 5, which shows the situation for $i_0 + i_1 + i_2 = 3$. The meaning of the small circles in the diagram is the following: For all triples (i_0, i_1, i_2) of nonnegative integers with $i_0 + i_1 + i_2 = n$ there is a basis function. If we arrange $(n+1) + n + (n-1) + \ldots + 1$ circles line by line in a triangular shape, like in Fig. 5, each circle corresponds to a basis function. The bottom line has $i_2 = 0$, the next one $i_2 = 1$, and so on. The different regions in the plane where the barycentric coordinates x_0, x_1, x_2 take different signs, lead to different sign distributions of the basis polynomials. Filled circles correspond to positive signs.

Tensor product surfaces

Assume that basis functions A_i, and B_j define two curve schemes. As already mentioned, the tensor product surface scheme defined by the two curve schemes is given by basis functions $A_i \cdot B_j$, and the linear combination $K = \sum_{i,j} K_{ij} A_i(u) B_j(v)$ has support function $s(n) = \sum_{i,j} s^\star_{ij}(n) A_i(u) B_j(v)$, where $s^\star_{ij}(n) = s_{ij}(n)$ if $A_i(u)B_j(v)$ is positive, and $-s_{ij}(-n)$ if not. As an example, Figure 6 shows in a symbolical way the sign distribution of TP Bézier functions. The interpretation of the figure is analogous to Fig. 5.

2.3 Envelopes of families of convex bodies

In the previous section we showed how to compute the locus $K(t)$ of curve points for a fixed parameter value t. This

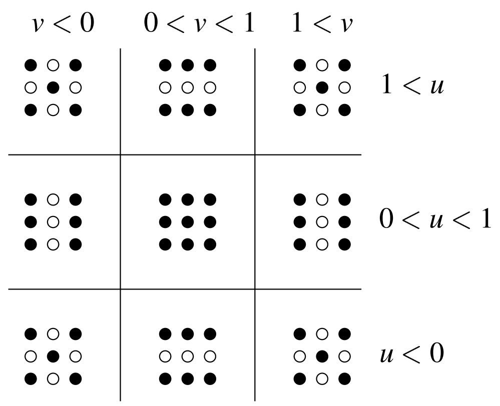

Figure 6: Distribution of signs of TP Bernstein polynomials $B_i^n(u) \cdot B_j^m(v)$

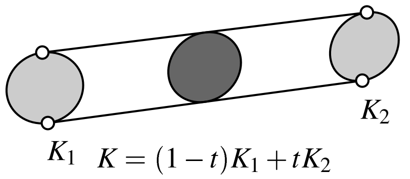

Figure 7: Common tangents of convex combination of convex bodies

was a certain affine or convex combination of convex domains. In this section we study the set which is traced out by $K(t)$ if t runs in its parameter interval (the gray area in Figures 2, 3, and 4). In some cases we are able to determine the boundary curve of this set.

Curves

We consider a Bézier curve $b(t) = \sum b_i B_i^n(t)$. If the b_i range independently in convex bodies K_i, then $b(t)$ ranges in the convex body $K(t) = \sum B_i^n(t) K_i$, whose support function can be computed by the algorithms given above. We describe the domain in space traced out by the movement of $K(t)$ in more detail.

First we consider the following situation: If $K = (1-t)K_1 + tK_2$, then the common tangent hyperplanes of K_1, K_2 are also tangent hyperplanes of K (see Fig. 7). They correspond to values $s_1(n) = s_2(n) = s(n)$ of the support functions of K_1, K_2, K, respectively.

The envelope of a convex body $K(t)$ which changes with time can be described in terms of the support functions $s(t,n)$ of $K(t)$. The common tangent hyperplanes of $K(t)$ and $K(t+\Delta t)$ correspond to normal vectors $n \in S^{d-1}$ with $s(t,n) = s(t+\Delta t, n)$, or

$$\frac{s(t+\Delta t, n) - s(t,n)}{\Delta t} = 0.$$

The limit $\Delta t \to 0$ gives

$$\frac{\partial}{\partial t} s(t,n) = 0.$$

In case of a Bézier curve, we are able to explicitely describe the tangent hyperplanes of the envelope. On the one hand, we have $\frac{d}{dt}(\sum_{i=0}^n b_i B_i^n(t)) = n \sum_{i=0}^{n-1} (b_{i+1} - b_i) B_i^{n-1}(t)$, so the normal vectors corresponding to the envelope's tangent hyperplanes are the zeros of the function

$$\frac{\partial}{\partial t} \sum s_i^\star(n) B_i^n(t) = n \sum_{i=0}^{n-1} B_i^{n-1}(t)(s_{i+1}^\star(n) - s_i^\star(n)).$$

On the other hand, we consider the two convex bodies

$$K_-(t) = \sum_{i=0}^{n-1} B_i^{n-1}(t) K_i, \qquad K_+(t) = \sum_{i=1}^{n} B_i^{n-1}(t) K_i.$$

Then $K(t) = (1-t)K_-(t) + tK_+(t)$ (see Fig. 2). The corresponding support functions shall be denoted by $s(t,n) = (1-t)s_-(t,n) + ts_+(t,n)$. The common tangent hyperplanes of $K_-(t)$ and $K_+(t)$ correspond to normal vectors $n \in S^{d-1}$ which fulfill $s_-(t,n) = s_+(t,n)$, which is equivalent to

$$s_-(t,n) = \sum_{i=0}^{n-1} s_{i+1}^\star(n) B_i^{n-1}(t) = \sum_{i=0}^{n-1} s_i^\star(n) B_i^{n-1}(t) = s_+(t,n)$$

and we see that it is equivalent to the previous condition that n defines a tangent hyperplane of the envelope. Thus we have shown the following

Proposition. *The domain traced out by $K(t)$ is the envelope of the common tangent hyperplanes of the convex bodies $K_-(t)$ and $K_+(t)$ which correspond to intermediate points in the recursive construction of a Bézier curve by the algorithm of P. de Casteljau by successive convex combinations (see Fig. 2).*

Another fact follows easily: For all points p contained in the envelope of the sets $K(t)$ we can explicitely find points b_i in the domains K_i together with a parameter value t such that the curve (c) with control points b_i assumes the value $p = c(t)$ — we have to choose the b_i such that there is a supporting plane for K_i which contains b_i and whose normal vector is also orthogonal to the envelope at p. This shows again that this method gives not only an estimate, but the exact locus of curves defined by control points varying in the convex domains K_i.

Surfaces

It is easy to extend the results of the previous paragraph to surfaces: all Bézier surfaces (triangular and TP-rectangular) contain Bézier curves. A hyperplane is tangent to the enveloping surface of a family of convex bodies $K(u,v)$ if and only if it is tangent to the envelope of two linearly independent one-parameter families $K(u(t),v(t))$.

Without going into detail, this shows the following: For TP surfaces and triangular surfaces, there is the algorithm of de Casteljau, which recursively evaluates the surface at certain parameter values by repeated convex combinations of the control points. The last step of this algorithm produces points, which span the tangent hyperplane of the surface at the point eventually constructed in the very last step. Now the tangent hyperplanes of the envelope, which are also tangent to $K(u,v)$, are precisely the common tangent hyperplanes of the convex bodies which correspond to these points.

2.4 Special Cases

'Interval' curves and surfaces

If the coordinates of control points are known to lie in certain intervals, then an equivalent formulation of this is that the control point itself varies in some orthogonal parallelotope whose faces are parallel to the coordinate hyperplanes. If the dimension is 2, this can be expressed by saying that interval bounds on the coordinates of points are the same as rectangular domains where the points themselves must be contained.

Interval curves and surfaces are not new: for instance interval Bézier curves are studied in [15, 16], and interval B-splines and their applications to curves and surfaces are described in [7, 8, 17, 18, 19].

The procedure of linear combination, especially of convex combination, of such parallelotopes again produces convex orthogonal parallelotopes. If the linear combination is with nonnegative factors, then the coordinates of the faces of the box containing the eventual curve or surface point can be computed by the *same* linear combination.

The support function of an orthogonal parallelotope is easily calculated: If the parallelotope in $\mathbb{R}^d$ has the equation $a_1 \le x_1 \le b_1, \dots, a_d \le x_d \le b_d$, and $n = (x_1, \dots, x_d)$, then let $p_i(n) = a_i$ if $x_i \le 0$ and $p_i(n) = b_i$ if $x_i > 0$. The function $s(n) = p_1(n)x_1 + \cdots + p_d(n)x_d$ then is the support function of the parallelotope. Fig. 4 shows an example of an interpolating 'interval' spline curve ($d = 2$).

'Disk' curves and surfaces

Another class of convex bodies closed under the operation of linear combination are the Euclidean balls of radius r, which in dimension one coincide with the intervals, and which in dimension two are usually called disks. If the linear combination of control points which yields the eventual curve/surface point is nonnegative, then both the midpoint and the radius of the eventual balls is obtained by the *same* linear combination of the midpoints and radii of the control point balls, respectively. Planar 'disk' Bézier curves are studied in [11].

3 Circles in plane and space

In this section we study a geometric problem of Euclidean geometry: the circumcircle of three points. It occurs e.g. in the construction of a Delauny triangulation. It turns out that the problem is more complicated than the affinely invariant problems of the previous section, and we will not study it in its maximum possible generality.

We describe the set of circles in the Euclidean plane which meet three three circular disks K_1, K_2, K_3. The geometric setting where this type of problem is most easily studied is Laguerre geometry (see [12, 20]). Here we use only elementary concepts, such as oriented circles and oriented contact.

Cycles

An *oriented circle* or *cycle* C is defined by its center $m = (m_1, m_2)$ and a radius r which can be any real number. The ordinary circle $|C|$ defined by C has center m and radius $|r|$. If $r = 0$, then $|C|$ is a point. Two cycles $C = (m_1, m_2, r)$, $C' = (m_1', m_2', r')$ are in *oriented contact*, if

$$d(C,C') = (m_1 - m_1')^2 + (m_2 - m_2')^2 - (r - r')^2 = 0 \quad (1)$$

(see Fig. 8). Obviously a cycle C of zero radius is in oriented contact with another cycle C', if the point $|C|$ is contained in $|C'|$. If all radii are nonzero and C, C' are in oriented contact, then $|C|$ touches $|C'|$.

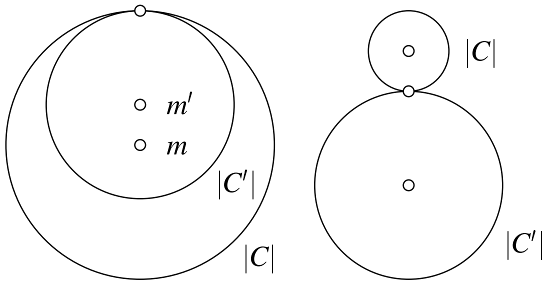

Figure 8: Cycles C, C' in oriented contact. Left: $rr' > 0$. Right: $rr' < 0$.

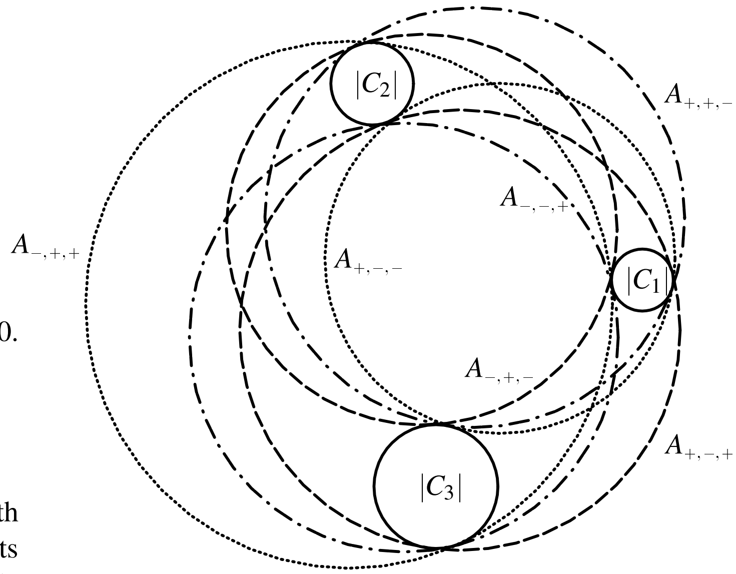

Figure 9: Six Apollonius circles defined by circles $|C_1|, |C_2|, |C_3|$.

The cyclographic model

We identify a cycle with center (m_1, m_2) and radius r with the point (m_1, m_2, r) of $\mathbb{R}^3$. This interpretation of points of $\mathbb{R}^3$ as cycles is called the *cyclographic model* of circle geometry. Lines and planes in $\mathbb{R}^3$ in this way correspond to certain sets of cycles, which are called *lines* or *planes*, or one- and two-parameter *linear families* of cycles.

The pseudo-euclidean squared distance $d(C, C')$ defined by Equ. (1) stems from the scalar product

$$\langle (x_1, x_2, x_3), (x_1', x_2', x_3') \rangle = x_1 x_1' + x_2 x_2' - x_3 x_3' \qquad (2)$$

via $d(C, C') = \langle C - C', C - C' \rangle$.

We call lines $p + \mathbb{R}v$ in $\mathbb{R}^3$ *steep* or *time-like*, if $\langle v, v \rangle < 0$, *light-like* or *ideal* if $\langle v, v \rangle = 0$, and *space-like*, if $\langle v, v \rangle > 0$. A plane (i.e., a two-parameter linear family of cycles) is called space-like if it contains only space-like lines (i.e., one-parameter families).

Two cycles $C = (m_1, m_2, r)$ and $C' = (m_1', m_2', r')$ span a steep line, if the distance of centers is less than the difference of radii. Their span is space-like, if the opposite inequality holds. Their span is light-like if they are in oriented contact.

Obviously affine transformations which preserve the squared distance (1) (or the scalar product (2), which is the same), preserve oriented contact of cycles. Such transformations do not change the type of lines and map space-like planes onto space-like planes.

The Apollonius problem

We want to find cycles C which are in oriented contact with *three* given cycles C_1, C_2, C_3. This problem is named after Apollonius of Perga and is easily solved with the cyclographic interpretation. Without going into detail, we describe a solution: Consider the plane $\varepsilon = [C_1, C_2, C_3]$. Choose the coordinate system in $\mathbb{R}^2$ such that ε contains the x_1-axis of $\mathbb{R}^3$. If ε is space-like, its slope equals $\tanh 2t$ for some t, and its points can be written in the form $(x_1, \alpha\cosh 2t, \alpha \sinh 2t)$. With the vector $n = (0, \sinh t, \cosh t)$ we define the affine mapping $\sigma : x \mapsto x - 2\langle n, x\rangle / \langle n, n\rangle \cdot n$ which transforms ε to the x_1x_2-coordinate plane, and which preserves oriented contact. It transforms C_1, C_2, C_3 to cycles C_1', C_2', C_3' of zero radius. Assume that the circumcircle of the points $|C_1'|$, $|C_2'|$, $|C_3'|$ has center $m' = (m_1', m_2')$ and radius r'. Then $A^+ = (m_1', m_2', r')$ and $A^- = (m_1', m_2', -r')$ are two cycles in oriented contact with C_i'. Because σ is its own inverse, $\sigma(A^+)$ and $\sigma(A^-)$ are in oriented contact with C_1, C_2, C_3.

This shows that there are up to eight solutions to the problem of finding circles which touch three given circles. They are found by assigning arbitrary orientations and applying the procedure described above. Fig. (9) shows an example and six solutions $A_{+,+,-}, \ldots$ The three signs show the sign of the radius of the circles C_1, C_2, C_3 such that the (positively oriented) solution cycle is in oriented contact with them.

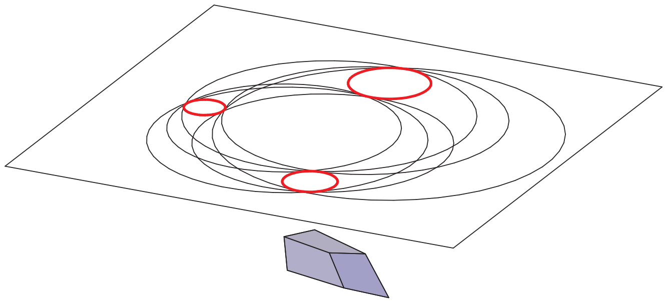

Figure 10: The curvilinear cube which is defined by three disks.

Cyclographic image of all circles passing through three disks

Assume three circular disks K_i in the plane which are disjoint. They are bounded by three circles $|C_1|$, $|C_2|$, $|C_3|$, where all C_i have nonnegative radius. The cycle with the same center but opposite radius will be denoted by C_i^-. To emphasize that the radius is nonnegative, we write C_i^+ for C_i. Because the disks K_i are disjoint all linear families (i.e., lines) spanned by C_i^+, C_j^+ or C_j^+, C_j^- are space-like.

If $X = X^+$ is a further cycle with nonnegative radius, then it is easy to see that $|X|$ intersects $|C_1|$ if and only if the line $X^+C_1^-$ is time-like and the line $X^+C_1^+$ is space-like, which means $d(X^+, C_1^-) \leq 0$ and $d(X^+, C_1^+) \geq 0$.

Thus the set of positively oriented cycles X^+ which intersect all three disks K_1, K_2, K_3 is given by the inequalities

$$\begin{array}{lll} d(X^+,C_1^-) \leq 0, & d(X^+,C_2^-) \leq 0, & d(X^+,C_3^-) \leq 0, \\ d(X^+,C_1^+) \geq 0, & d(X^+,C_2^+) \geq 0, & d(X^+,C_3^+) \geq 0. \end{array}$$

It is depicted in Fig. 10 together with the three disks and six of the eight Apollonius circles, and looks like a curvilinear cube, whose faces, edges, and vertices correspond to cycles which touch one, two, or three boundary circles C_i^+, C_i^-, respectively. The eight vertices correspond to the eight solutions of the Apollonius problem (there are eight solutions, because the planes spanned by three boundary cycles are space-like for all possible sign combinations).

Lines which meet three disks

If three circular disjoint disks K_1, K_2, K_3 in the plane are given, it may happen that a straight line meets all three of them. We want to characterize this situation in terms of the cyclographic model. To each K_i there correspond two cycles C_i^+ and C_i^- like in the previous paragraph. The plane spanned by C_1^+, C_2^+, C_3^- will be denoted by ε_{++-}, and analogously for the other sign combinations.

Proposition. *No line which meets all three disks K_i, if and only if all planes ε_{++-}, ε_{+-+}, ε_{-++} are space-like.*

To prove this we assume that a line meets K_1, K_2, K_3. Then there is a line L which touches the boundary of two disks and still intersects the third. Without loss of generality we assume that L touches $|C_1|$ and $|C_2|$, and intersects K_3. If K_1, K_2 are on the same side of L, we let $C_1 = C_1^+$, $C_2 = C_1^+$, otherwise we give different signs and let $C_1 = C_1^+$, $C_2 = C_1^-$. Among the elements of the linear family spanned by C_1, C_2 there is a cycle C such that $|C|$ intersects K_3. If we give C, C_3 opposite signs we see that $d(C, C_3) \leq 0$, and the span of C, C_3 is time-like. This shows that the plane spanned by C_1, C_2, C_3 is not space-like. If all C_i happen to the have the same sign, then we may reverse one of them, and the plane cannot become space-like because its slope increases by this operation. If we have two minus signs, we reverse all signs, and the type of the plane does not change. This shows the 'if' part of the statement. The 'only if' part is similar.

Cyclic regions in the plane

The set of all cycles X which are in oriented contact with *two* cycles C_1, C_2 obviously is given by the equations $d(X, C_1) = d(X, C_2) = 0$. Subtracting these two quadratic equations gives a linear one, namely

$$\langle X - \frac{1}{2}(C_1 + C_2), C_1 - C_2 \rangle = 0$$

which is the symmetry plane of C_1, C_2 (the symmetry is in the sense of the pseudo-euclidean scalar product given by Equ. (2)). If $M = \frac{1}{2}(C_1 + C_2)$ then the lines MX and C_1C_2 are orthogonal in the sense of the scalar product (2). Pythagoras' theorem now says $d(C_1, X) = d(X, M) + d(C_1, M)$ which means that $d(X, M) = -d(C_1, M) = \text{const.}$

This shows that this set $\mathcal{C}$ of cycles is contained in a two-parameter family (i.e., a plane) and has constant distance from a point M of this plane. It is therefore called a *circle* of cycles. The union of all $|X|$ for $X \in \mathcal{C}$ is called a *cyclic region*. $\mathcal{C}$ is called space-like, if its carrier plane is.

Inversions

The mapping which transforms a point x in the plane to $q+(x-q)/\|x-q\|^2$ is called an *inversion* with center q. It is well known that it transforms circles to circles, except for the circles which contain the origin, which will be transformed to lines.

This motivates to define the following mapping of cycles: A cycle $X=(m_1,m_2,r)$ is mapped according to

$$\mathrm{inv}_Q : X \mapsto X + \frac{X-Q}{\langle X-Q, X-Q\rangle}, \qquad (3)$$

where $Q=(q_1,q_2,0)$. This mapping maps points (i.e., cycles of zero radius) like the ordinary inversion, and it preserves oriented contact. It is an easy exercise to see that this mapping actually describes the action of the inversion on cycles.

The mapping inv_Q is undefined for cycles which are in oriented contact with the center Q. It is well known that it transforms a circle $\mathcal{C}$ of cycles to a space-like circle of cycles, if and only if no $X \in \mathcal{C}$ is in oriented contact with the inversion center Q (i.e., the point $|Q|$ is contained in no $|X|$ for $X \in \mathcal{C}$).

Circles which meet three disks — the fat circle

We resume the discussion of the set of cycles C which meet three disjoint circular disks K_1,K_2,K_3. We have already described this set by distance inequalities. We now want to describe the union of circles $|C|$.

We consider the eight solution circles of the Apollonius problem for the circles $|C_1|,|C_2|,|C_3|$. If we choose three orientations, e.g., $C_1=C_1^+$, $C_2=C_2^-$, $C_2=C_3^+$, there are two *cycles* which are in oriented contact with C_1,C_2,C_3. The cyclic region defined by them is denoted by R_{+-+}, and the corresponding circle of cycles by $\mathcal{C}_{+-+}$. We can do the same for all other sign combinations also. Obviously reversion of all signs does not change the cyclic region.

Proposition. *The union of all circles which meet three disks is given by*

$$R_{++-} \cup R_{+-+} \cup R_{-++}.$$

This set will be called a 'fat circle'.

Proof: Suppose a point $x=(x_1,x_2)$, which will be identified with the cycle $X=(x_1,x_2,0)$, is not contained in R_{++-}. Then the inversion inv_X maps $\mathcal{C}_{++-}$ to a space-like circle

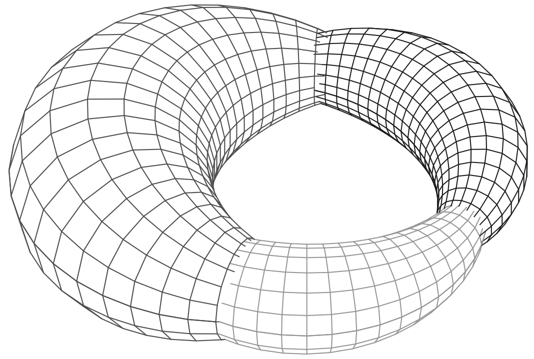

Figure 11: Circles which meet three balls

$\mathcal{C}'_{++-}$ of cycles. In the plane inv_X acts like the ordinary inversion, and so any circle containing x is mapped to a straight line, which intersects the disks $\mathrm{inv}_X(K_1)$, $\mathrm{inv}_X(K_2)$, $\mathrm{inv}_X(K_3)$. But we have already shown that this is impossible if all three carrier planes of C'_{++-}, C'_{+-+}, C'_{-++} are space-like. This shows the statement of the proposition.

Circles in space

Here we ask for circles which intersect three balls, bounded by spheres. Analogous to the planar case, we consider cycles, which are spheres of radius r and identify the set of cycles with $\mathbb{R}^4$. The distance and scalar product is modified in the obvious way.

A circle of cycles (cf. the definition of the planar version above) defines a cyclic region, which turns out to be a *Dupin cyclide*. This is a surface which is the envelope of oriented spheres whose centers are contained in a plane, and which are tangent to two oriented circles there (an example is the torus, see also [4]).

A procedure similar to the planar case leads to the conclusion that the set of circles which intersect three disjoint balls is bounded by three Dupin cyclides, which are found by intersecting the three balls with their symmetry plane, and defining the cyclic regions R_{++-}, R_{+-+}, R_{-++} for them, which are the intersections of the Dupin cyclides with this symmetry plane. Fig. 11 shows an example.

Extremal properties

We consider again three disjoint planar disks K_1, K_2, K_3 with centers m_1, m_2, m_3, and the set of circles which intersect all three of them. We restrict ourselves to the case of all K_i having equal radius r. Consider the three cyclic regions R_{++-}, R_{+-+}, R_{-++}, whose union is the fat circle. The Euclidean reflection which maps m_1 to m_2 is a symmetry of R_{++-}, and likewise the reflections which interchange the pairs m_1 — m_3 and m_2 — m_3 are symmetries of R_{+-+} and R_{-++}, respectively.

Consider the circumcircle $|C|$ of the centers m_1, m_2, m_3. The point of R_{++-} which has maximum distance δ from $|C|$ is one of the points where the symmetry line of m_1, m_2 meets R_{++-}'s boundary. If we fix the points m_1, m_3, and move m_2 towards a position which is symmetric with respect to the pair m_1, m_2, then δ increases.

There is such a maximal deviation for all three cyclic regions, and clearly the smallest value of the greatest δ is attained if each of the centers m_1, m_2, m_3 is in symmetric position with respect to the other two, which means that m_1, m_2, m_3 are the vertices of an equilateral triangle.

Conclusions

In the first part of the paper we studied affine and convex combinations of points from the viewpoint of error propagation. An affine or convex combination of points which are known to be contained in certain convex domains, is itself contained in an appropriate combination of these domains. This leads to precise bounds for Bézier and spline curves with toleranced control points.

The second part of the paper deals with a geometric construction of Euclidean geometry: the circumcircle of three points. If these three points are known to be contained in three disks, then the circumcircle is known to be contained in the union of three cyclic regions, which are found by solving the Apollonius problem for the three given disks.

The aim of the paper on the one hand was to show how to treat geometric constructions of affine and Euclidean geometry, and on the other hand to demonstrate how much more difficult error propagation problems become if one uses a richer geometry such as the Euclidean one compared to planar affine geometry.

Acknowledgements

This work was supported in part by the Lithuanian Foundation of Studies an Science.

References

[1] M. Aichinger. A Collision Problem for Worst Case Tolerance Objects. Dissertation, Linz 1996.

[2] S. L. Abrams, W. Cho, C.-Y. Hu, T. Maekawa, N.M. Patrikalakis, E.C. Sherbrooke, X. Ye. Efficient and reliable methods four rounded-interval arithmetic. Computer-Aided Design 1998;30, 657–665.

[3] C. de Boor. A Practical Guide to Splines. Springer Verlag, New York 1978.

[4] D. Dutta, R. R. Martin, M. J. Pratt. Cyclides in surface and solid modeling. IEEE Comp. Graphics and its Applications 1993;13, 53–59.

[5] R. Farouki, T. Goodman: On the optimal stability of the Bernstein basis. Mathematics of Computation 1996;216, 1553–1566.

[6] C. U. Hinze. A Contribution to Optimal Tolerancing in 2-Dimensional Computer Aided Design. Dissertation, Linz 1994, declassified 1999.

[7] C.-Y. Hu, T. Maekawa, E. C. Sherbrooke, N. M. Patrikalakis. Approximation of measured data with interval B-splines. Computer-Aided Design 1997;29, 791–799.

[8] C.-Y. Hu, T. Maekawa, N. M. Patrikalakis, X. Ye. Robust interval algorithm for surface intersections. Computer-Aided Design 1997;29, 807–817.

[9] P. Gruber, J. Wills. Handbook of Convex Geometry (2 volumes). North Holland, Amsterdam 1993.

[10] I.-K. Lee, M-S. Kim, G. Elber. Polynomial/rational approximation of Minkowski sum boundary curves. Graphical Models and Image Processing 1998;60, 136–165.

[11] Q. Lin, J. Rokne: Disk Bézier curves. Comp. Aided Geometric Design 1998;15, 721–737.

[12] H. Pottmann, M. Peternell. Applications of Laguerre Geometry in CAGD, Comp. Aided Geometric Design 1998;15, 165-186.

[13] A. A. G. Requicha. Towards a theory of geometry tolerancing. Int. J. of Robotics Research 1983;2, 45–60.

[14] L. Schumaker. Basic Spline theory. Wiley, 1981.

[15] T. W. Sederberg and R. T. Farouki. Approximation by interval Bézier curves. IEEE Computer Graphics 1992;12, 87–95.

[16] T. W. Sederberg and D. B. Buehler. Offset of polynomial Bézier curves: Hermite approximation with error bounds. in *Mathematical Methods in Computer Aided Geometric Design, Vol. II*, T. Lyche and L. Schumaker Eds., Academic Press, 1992, pp. 549–558.

[17] G. Shen, N. Patrikalakis. Numerical and Geometric Properties of Interval B-Splines. *Int. J. Shape Modeling*, 1998;4, 31–62.

[18] S. T. Tuohy, T. Maekawa, G. Shen, N. M. Patrikalakis. Representation of geophysical maps with uncertainty. in: *Communicating with Virtual Worlds*, Proc. of CG International '93, N. M. Thalmann and D. Thalmann, Eds., Springer, Tokyo, 1993.

[19] S. T. Tuohy and N. M. Patrikalakis. Nonlinear data representation for ocean exploration and visualization. Journal of Visualization and Computer Animation 1996;7, 125–139.

[20] R. Krasauskas, C. Mäurer. Studying Cyclides with Laguerre Geometry. to appear in *Comp. Aided Geometric Design*.

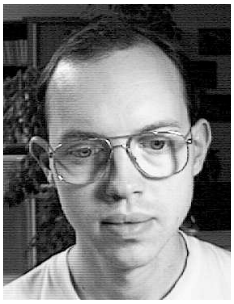

Johannes Wallner is a member of the mathematics department at the University of Technology in Vienna, Austria. He received his PhD in 1997. His research interests include geometry and its applications to Computer Aided Geometric Design. Copies of recent publications can be downloaded from *http://www.geometrie.tuwien.ac.at/ wallner*

Rimvydas Krasauskas is an associate professor in the Department of Mathematics and Computer science, Vilnius University, Lithuania. His current research interests are in geometry of real rational surfaces and their applications in computer aided geometric design. He graduated from Moscow State University in 1982, where he studied computer science and numerical mathematics. In 1988 he received a Ph.D. in pure mathematics (algebraic topology). Since then he has been the head of the chair Geometry and Topology at Vilnius university. The change from algebraic topology too CAGD in the period of 1994–96 was partially supported by an American Mathematical Society grant for fSU.

Helmut Pottmann is professor of geometry at the University of Technology in Vienna, Austria. His research interests include classical geometry and its applications, especially to Computer Aided Geometric Design, kinematics, and the relations between geometry, numerical analysis and approximation theory. A list of recent publications can be found at *http:// www.geometrie.tuwien.ac.at/pottmann*